Andean Geology 53 (3): 627-642. September, 2026
doi: 10.5027/andgeoV53n3-3815

Andean Geology
www.andeangeology.cl

Thermal contraction and expansion of quartz and its role in porphyry deposit mineralisation: A review

***Eduardo A. Rossello[1], Adrián H. Gallardo[2]**

[1] *IGEBA-CONICET - Departamento de Ciencias Geológicas, University of Buenos Aires, C1428EHA, Buenos Aires, Argentina.*
ea_rossello@yahoo.com.ar

[2] *AHS Consulting, Stirling 6017, Western Australia.*
adgallardo@geowater.com.au

* *Corresponding author: ea_rossello@yahoo.com.ar*

ABSTRACT. Porphyry deposits are strongly associated, both spatially and temporally, with acid to meso-silicic intrusions. However, the mechanisms responsible for low-grade, large-volume mineralisation are not yet fully understood. Considering the relative thermal expansivity of key rock-forming minerals, measurements of their volumetric and morphological changes are critical to understanding the factors that control the emplacement of disseminated mineralisation. This study reviews the character and influence of differential thermal expansion between quartz and feldspar in porphyry deposits, with particular emphasis on the volumetric changes occurring at the α-β quartz transition. In a typical meso-silicic rock, expansion can reach approximately 1.2%. In addition, microfracturing and thermally induced openings can significantly enhance the transport and dissemination of late-stage mineralising fluids, with degassing resulting from thermal expansion further contributing to fluid enrichment and differential mineral deposition.

Keywords: Quartz, Thermal expansion-contraction, Cracking, Mineralisation, Porphyries.

RESUMEN. Contracción y expansión térmica del cuarzo y su rol en la mineralización de depósitos tipo pórfido: una revisión. Los depósitos tipo pórfido están estrechamente asociados, tanto espacial como temporalmente, con intrusiones ácidas a mesosilícicas. Sin embargo, los mecanismos responsables de la mineralización de baja ley y gran volumen aún no se comprenden por completo. Considerando la expansividad térmica relativa de minerales formadores de roca clave, la medición de sus cambios volumétricos y morfológicos resulta fundamental para comprender los factores que controlan el emplazamiento de la mineralización diseminada. Este estudio revisa la naturaleza e influencia de la expansión térmica diferencial entre cuarzo y feldespato en depósitos de pórfido, con especial énfasis en los cambios volumétricos que ocurren durante la transición α-β del cuarzo. En una roca mesosilícica típica, la expansión puede alcanzar aproximadamente el 1,2%. La microfracturación y las aberturas inducidas térmicamente pueden mejorar significativamente el transporte y la diseminación de fluidos mineralizantes en etapas tardías, mientras que la desgasificación resultante de la expansión térmica puede contribuir aún más al enriquecimiento de fluidos y a la depositación mineral diferencial.

Palabras clave: Cuarzo, Expansión-contracción térmica, Agrietamiento, Mineralización, Pórfidos.

1. Introduction

Porphyry deposits, which are currently the world's largest copper resources hosting Cu-Fe sulfides, have a strong spatial and temporal association with dioritic to granitic intrusions (*e.g.*, Sillitoe, 2010). These deposits occur both in thick continental and thin oceanic arcs at depths between ~1 and ~6 km above parental magma chambers (*e.g.*, Chiaradia, 2022). There is a very extensive literature on the genesis of porphyry systems and their alteration stages, with Phillips *et al*. (2023) providing a comprehensive summary of the key factors contributing to porphyry deposit formation.

Hydrothermal processes are typically emphasised as a primary mechanism of mineralisation, noting the strong partitioning of both Cu and Au into high-temperature, oxidising, high-salinity hydrothermal fluids. Of particular relevance to the present work, due to its similarity to an analysis of mineralisation related to tectonic mechanisms, Phillips *et al*. (2023) proposed that mineralised quartz veins are due to the injection of fluids during the hydraulic fracturing of the host intrusions once these stocks cooled significantly below their solidus temperature. Fluid-rock interactions that mobilise dissolved ions can lead to spatially predictable hydrothermal alteration and mineralisation distributions (*e.g.*, Sillitoe, 2010). Typically, alteration zones display a characteristic pattern, with potassic alteration dominating the deeper and central regions. Moving outwards and/or upwards, this zoning transitions through chlorite-sericite to sericite alteration, and further into (advanced) argillic or propylitic assemblages (*e.g.*, Seedorf *et al*., 2005; Zhang *et al*., 2025).

As stated by Misra (2000) and Phillips *et al*. (2023), porphyry deposits refer to large, relatively low-grade, epigenetic, intrusion-related vein-network mineralisation (stockwork) and surrounding alteration that can be exploited by bulk-mining techniques. Despite the invariable association of these textures with porphyry-style mineralisation, the controls on the stockwork dissemination remain unclear (*e.g.*, McMillan and Panteleyev, 1998). This could be attributed to either the small size (often less than several centimetres) of the stockworks, or due to overprinting of several magmatic and hydrothermal stages as well as different pulses of alteration (*e.g.*, Seedorff *et al*., 2008; Carter and Williamson, 2022).

The genesis of large-scale mineralisation disseminated in fine and local veins and inclusions has typically been associated to microfracturing (*e.g.*, Guilbert and Park, 2007). As a result, advected ore metals are accumulated in a downward-growing ore shell influenced by a steep P-T gradient (*e.g.*, Heinrich, 2024). In particular, it is widely accepted that the mineralisation occurs over short geological times, where deposition from metal-rich fluids is rapidly followed by additional tectonic stresses. For instance, Stanton-Yonge *et al*. (2025) documented a full cycle of fluid overpressure build-up, migration, and pressure release through small seismic events accompanied by swarm-like microfracturing. Similarly, Xu *et al*. (2025) showed that episodic hydrothermal pulses not only drive mineral growth but also induce stresses that generate new fractures, thereby enhancing permeability and facilitating the continued migration of ore-forming fluids. Similar to observations by Boulogne *et al*. (2026), the above controls are even more critical in epigenetic deposits, where the structure is the main factor determining the circulation, precipitation, and in many cases the generation of hydrothermal solutions that are associated with mineral deposits and/or their alterations. Therefore, a more accurate knowledge of the structural control, geometric configuration, and internal architecture of the mineralised bodies of a given deposit is important to not only understand ore-forming events (Fridovsky *et al*., 2023), but to guide the prospecting and exploration of economic minerals (Guilbert and Park, 2007; Smirnov, 1976).

Plutonic rocks are crystalline and typically contain >60% silica. Therefore, any potential volumetric changes are broadly related to their silica content, mostly present within quartz and feldspar minerals (Burnham and Ohmoto 1980). While there is abundant literature on mineral thermal properties, only a handful of studies will be mentioned here, giving preference to those about quartz. Raman and Nedungadi (1940), for instance, indicated that the thermal expansion coefficient of quartz gradually increases over the 200-573 °C range, becoming theoretically infinite at the transition point and then suddenly dropping to negative values. Changes in cooling temperature can potentially affect the mechanical properties of minerals, leading to microcracking due to mismatches in the coefficients of thermal expansion (Bauer and Johnson, 1979). Vázquez *et al*. (2015) found that these thermally induced microcracks may subsequently coalesce and propagate into macrocracks. In this context, laboratory experiments by Johnson *et al*. (2021) demonstrated enhanced microcracking in rocks

as they cross the α-β quartz transition. In granites, microcracks would initiate at 300 °C and coalesce between 400 and 600 °C, inducing a decrease in rock strength (Xu *et al*., 2023), with cracks and small-scale microfractures propagating from 100 to 500 ºC (Dong *et al*., 2024). Finally, according to Brantley *et al*. (1990), macrofractures (*i.e*., visible to the naked eye) transport most of the fluids as they seal relatively slowly, whereas microcracks (*i.e*., millimetre scale or smaller) are typically responsible for the pervasive penetration of fluids into the mass rock.

The aforementioned studies and many others have contributed to a better understanding of the influence of temperature changes on rock mechanical properties. However, there are still uncertainties in relation to mechanical failure and the development of microfractures due to thermal stress on mineral particles within the rock. Intra-grain displacements and the initiation of microcracks caused by thermal stress are also poorly known.

Differential thermal expansion between quartz and other key, major rock-forming minerals, particularly feldspars, can lead to non-uniform rock volume changes. Accordingly, the present study investigates the influence of thermal processes, specifically the differential contraction and expansion of quartz during cooling in relation to other key rock constituents, on the genesis, transport, and emplacement of disseminated mineralising fluids in mesosilicic intrusives. We first review some fundamental thermal-expansion characteristics of major minerals to then investigate its influence on rock failure and the emplacement of disseminated mineralisation in porphyry settings.

2. Geological considerations

2.1. Porphyry deposits

Magmatic rocks are the most important components of the continental crust (Streckeisen, 1974). These lithologies are associated with various types of hydrothermal mineralisation as well as disseminated mineral deposits originated from the cooling processes. Porphyry deposits are formed by fluids released from felsic magmatic intrusions of batholitic dimensions (*e.g*., Korges *et al*., 2020). Porphyry deposits share several common characteristics, including large tonnage with low grades, intrusion-related emplacement, formation at paleodepths of 1.5-4 km or greater, hydrothermal alteration, fracture- and vein-controlled mineralisation, and associations with breccias and stockworks (Sillitoe, 2000, 2010; Seedorff *et al*., 2005). In addition, crypto-explosive breccias or crypto-explosive breccia pipes are often spatially, temporally, and genetically linked to many porphyry deposits (Xu *et al*., 2022). In this context, fluids migration and mineral deposition can be associated to several factors such as rock mechanical breaking, brecciation, grains' rearrangements and thermally induced microfracturing.

Fluids transport and the subsequent rock alteration and mineral deposition is typically largely controlled by an array of fissures and cracks, usually dichotomous and in random multi-scalar directions such as stockworks (Seedorff *et al*., 2005; Frenzel and Woodcock, 2014). The term stockwork specifically refers to a network of small-scale, closely spaced and randomly oriented veins occurring in localised swarms, making it necessary to mine the deposit by bulk-mining techniques. Stockwork veins are usually related to breccias, pipes and dykes, and in some cases, host high-grade mineralisation (Sinclair, 1995).

Mechanical failure and the development of fractures is widely attributed to the role of magmatic volatiles. Water entering micropores changes the composition and bond energy of minerals, resulting in increased micropores and weakened interlocking between grains (Ding and Tang, 2024). Over time, the magma pressure increases due to volatile exsolution from the melt as the magma reservoir cools, a process usually referred to as second boiling (Mittal and Richards, 2019). Upon cooling and crystallisation, the portion of volatiles in the melt that is not incorporated into newly formed minerals is liberated as a fluid phase (Burnham, 1979). Owing to the magma rise, vapor phases expand and provide the energy for tensile cracks and hydrofracturing of the rock. Such hydrofracturing occurs whenever the fluid pressure is greater than the hydrostatic pressure and tensile strength of the rock (Tosdal and Richards, 2001). In this regard, the magma moves upward into the fractured crust, releases volatiles, and depressurises, leading to the precipitation of minerals (Sillitoe, 2000; Seedorff *et al*., 2005).

Porphyry deposits are characterised by a zonation of mineralisation and associated types of hydrothermal alteration (*e.g*., Mavrogonatos *et al*., 2018). These alteration halos can extend for more than 5 km from the ore deposit itself, and the magmatic fluids are likely to contribute to its development even over such

large distances (Pacey *et al*., 2020; McCann, 2024). Laminated veinlets and fractures of cm- to dm-scale spacing are typical of the inner, highly mineralised, high-temperature potassic alteration zone. More distally, an argillic alteration halo commonly extends into the outer rock. In here, veins and veinlets tend to be wider, more continuous, more widely spaced, and more variable in strike and dip. Millimetre- to cm-wide cross-cutting quartz veins and veinlets also occur in a strongly altered quartz-sericite zone (Ruiz *et al*., 2005).

Cracks growth can also be affected by the grains' composition and the temperature distribution within the rock. Increasing temperature reduces the rock failure threshold and prolongs the propagation of cracks (Shao *et al*., 2015; Qiu *et al*., 2024). Thermal stresses are likely to be significant and sufficient to create an extensive fracture network around the magma body by brittle yielding (Kiss *et al*., 2023). In effect, thermal processes induce volume changes, which can evolve into a fracture network by mineral dissolution and crystallisation, grains' dislocation and rearrangement, hydraulic fracturing or thermal cracking on a cooling magma.

2.2. The thermal expansion of minerals

Dilatancy refers to changes of rock volume under differential stress or thermal variations. The generation of dilating spaces in the host rock is essential to facilitate the circulation and accumulation of mineralising fluids with economic potential (Rossello and López-Isaza, 2023). A higher temperature can potentially accelerate the dilatancy rate and increase the total volumetric expansion (Chen *et al*., 2019). In this regard, an overall increase in the rock volume corresponds to positive dilatancy or thermal expansion, whereas a reduction in volume refers to negative dilatancy or thermal contraction.

When a rock undergoes thermal changes, the different mineral constituents, each with different values of thermal expansion, create volumetric strains that may result in microfracturing and grains' realignment within the rock. In this context, temperature increase is the most relevant factor causing mineral transformations and bulk mechanical damage to rocks (Vázquez *et al*., 2021). Dilatancy can be generated by the differential thermal expansion exhibited by quartz grains relative to feldspars in the zone of quartz inversion (Skinner, 1966; Rossello, 2008). The thermal behaviour of quartz and feldspars is briefly explained below.

2.3. Quartz

Quartz exists in two polymorphs: α-quartz (trigonal, low-temperature) and β-quartz (hexagonal, high-temperature). α-quartz is stable below 573 °C but undergoes a phase transition to the β-polymorph at temperatures between 573 and 870 °C (Breuer and Schilling, 2021; Aoyagi and Takeda, 2022). The transition from α- to β-quartz is due to a modification of the atomic structure, leading to important changes in the optical, thermal and physical properties of the crystals (Rossello and Reynard, 1997). According to Rossello (2008), quartz shows two notable behaviours: 1) in the α-quartz field, thermal expansivity increases sharply as the temperature approaches the transition, and 2) in the β-quartz field, volume remains nearly constant at least up to about 800-870 °C (Fig. 1). This contrast results in significant volumetric variations at the transition temperature, with the *β* form having the larger volume (Johnson *et al*., 2021) (Fig. 1).

2.4. Feldspars

Feldspars are broadly classified into two major series: alkali feldspars, with orthoclase ($KAlSi_3O_8$) as the potassium-rich endmember, and plagioclase feldspars, with albite ($NaAlSi_3O_8$) and anorthite ($CaAl_2Si_2O_8$) as the sodium- and calcium-rich endmembers, respectively. The behaviour of feldspars is complex, as it is influenced by displacive and diffusive transformations as well as order-disorder transitions (Tribaudino *et al*., 2010). For alkali feldspars, the average coefficient of thermal expansion is approximately $2\pm0.5\times10^{-5}$ K^{-1} within the temperature range considered in this study (ambient to >900 °C; Hovis *et al*., 2010).

Albitisation significantly alters feldspar volume. According to Engvik *et al*. (2008), albitisation produces a volume decrease of ~7-9%, which results in stress accumulation and pervasive microfracturing. Similarly, Norberg *et al*. (2011) documented the pseudomorphic replacement of potassium feldspar by albite under conditions of 500 °C and 200 MPa, observing a ~7% molar volume decrease. This generated elastic strain at reaction fronts and porosity development. The Norberg *et al*. (2011) study demonstrated that

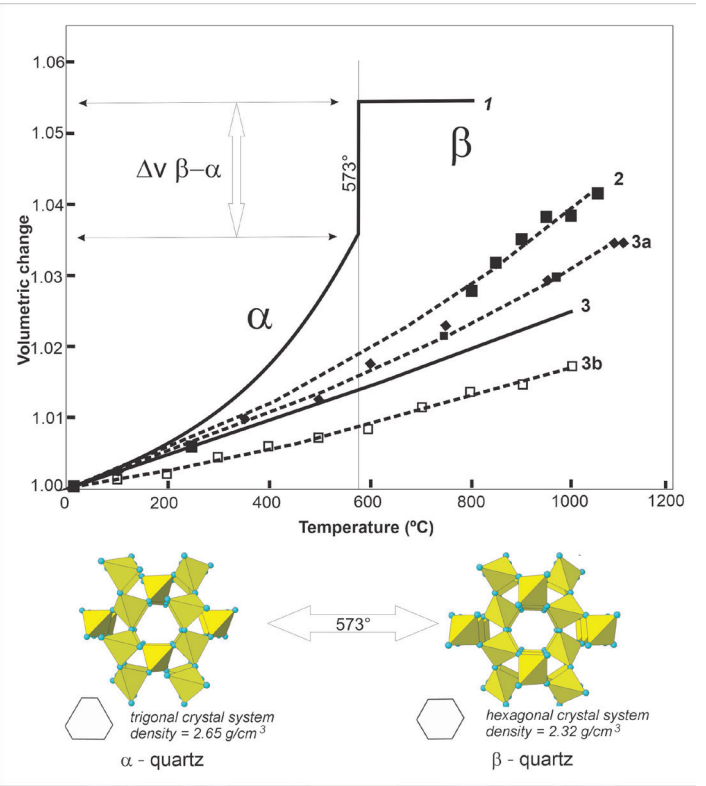


FIG. 1. Change in mineral volume vs. temperature (°C) at standard atmospheric pressure for: **1)** quartz (α and β forms); **2)** alkali feldspar (average orthoclase, microcline and sanidine); **3)** average plagioclase (3a: albite, 3b: anorthite). Below: schematic structures of α- and β-quartz. Diagram after Skinner (1966), Rossello and Reynard (1997), and Rossello and López-Isaza (2023).

interface-coupled dissolution-reprecipitation can lead to highly porous reaction rims and even visible cracks across mineral interfaces. For plagioclase feldspars, earlier studies (Kozu and Ueda, 1933; Skinner, 1966) reported that increasing anorthite content reduces the overall thermal expansion.

More recently, laboratory analyses by Sokolar and Nguyen (2024) confirmed that heating test samples induced localised crystallisation of anorthite, typically accompanied by minimal volume change. The mean coefficient of thermal expansion shows a systematic decrease from ~3.1×10^{-5} K^{-1} for low albite to ~0.9×10^{-5} K^{-1} for fully ordered anorthite (Henderson, 2021). Standard samples of low and high albite yielded thermal expansion coefficients of approximately 2.5×10^{-5} K^{-1}, a value that appears intrinsic to the mineral structure for a given degree of ordering. However, between 800 and 1050 °C, these same samples exhibit an increase in volume expansion (Fig. 1). Moreover, equilibrated albite specimens display greater expansion compared to unequilibrated albite, emphasising the influence of the structural state on thermal behaviour (Kroll, 1984).

3. Review

For simplicity purposes, the behaviour of minerals in a cooling felsic magma body considers the modelling of feldspars as a single phase controlled by their average thermal expansivity (*e.g.*, Rossello and Reynard, 1997; Vigneresse, 2007; Kumar, 2014). In this case, the thermal expansivity values were set to vary between 2.5×10^{-5} K^{-1}, representing an average of alkali feldspar and unequilibrated plagioclase, and 2.1×10^{-5} K^{-1}, corresponding to the equilibrium-order plagioclase, which reflects fully crystallised, compositionally stable plagioclase under equilibrium conditions.

There is a pronounced difference in the thermal expansion behaviour of quartz versus feldspars in

the temperature interval spanning the β-α quartz transition down to ambient conditions (Figs. 1 and 2). In the porosity vs. temperature curves (Fig. 2), three main trends can be observed below the β-α transition: 1) a steep increase in porosity immediately following the transition, reflecting the rapid volume change associated with the phase transformation inferred from the literature; 2) a moderate increase in porosity over the temperature range ~200-573 °C, corresponding to gradual thermal expansion and possible minor reactions in feldspars; and 3) relatively stable porosity behaviour at temperatures below ~200 °C, where both quartz and feldspars exhibit negligible thermal expansion and minimal porosity changes. Using this mechanism, and consistent with the trends seen in the curves, the maximum porosity

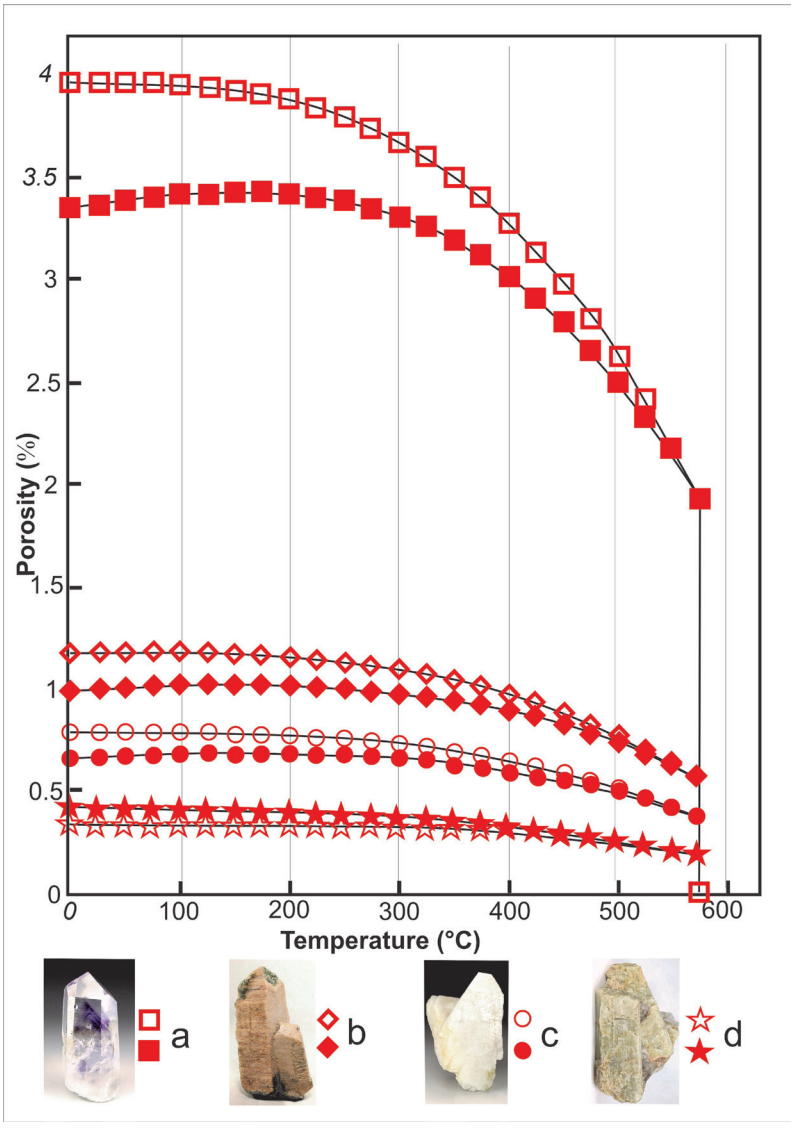


FIG. 2. Porosity (%) vs. temperature (°C) diagram. Porosity varies with temperature due to the different thermal expansion coefficients of minerals: (**a**) quartz, (**b**) alkali feldspar, (**c**) albite, and (**d**) anorthite. The maximum porosity ranges from about 0.4% in quartz-poor granitoids to 1.2% in typical felsic rocks, such as granites with ~30% quartz and abundant feldspars (from Rossello and López-Isaza, 2023). The open symbols (squares, diamonds, circles, and stars) are based on an average minimum thermal expansivity of 2.5×10^{-5} K^{-1} (averaging potassium feldspar and unequilibrated plagioclase). The closed symbols indicate a maximum thermal expansivity determined from equilibrated plagioclases (after Rossello and Reynard 1997).

observed in typical granites with ~30% quartz and abundant feldspars, reaches approximately 1.2% (Rossello and López-Isaza, 2023).

Rossello and Reynard (1997) proposed that granitoids under cooling conditions exhibit limited mechanical deformation, as the framework of feldspar crystals offsets the formation of voids. Consequently, changes in overall rock volume would be primarily governed by the thermal expansivity of the feldspar network, with the influence of accessory minerals (*e.g*., micas) being minimal due to their relatively low abundance. This conceptual model was supported by the experimental work of Jiang *et al*. (2022), who subjected granite specimens to cyclic heating (150-300 °C) followed by water cooling. They observed mechanical changes linked to microcrack development and thermal damage, yet the bulk mechanical response of the granite remained largely controlled by the feldspar assemblage. Further experimental insights from Sly *et al*. (2023) on the low-temperature plastic rheology of granitic feldspar and quartz reinforced the above conclusions, highlighting the role of feldspars in governing both elastic and semi-brittle deformation mechanisms at cooling temperatures.

Under ideal conditions, secondary porosity in rocks composed solely of quartz and feldspar may result directly from volume changes associated with the α-β phase transition in quartz and the differential thermal expansion of the mineral components (Figs. 1 and 2). Calculating this porosity requires knowing the initial volume occupied by β-quartz at a specific temperature within its stability field, which is influenced by the thermal expansivity of feldspar, and the intrinsic volume of quartz at each temperature, determined by its own thermal expansivity.

An important aspect that remains debated in the literature is how this mechanism interrelates with confining pressure and the viscoelastic response of the rock mass, given that its action could attenuate or neutralise the dilatancy produced (*e.g*., Heap *et al*., 2009; Brantut *et al*., 2013). Nonetheless, the assumptions discussed above are considered valid since the aim of this study is to estimate the maximum porosity associated with the differential thermal expansion between quartz and feldspars. In addition, feldspars constitute over 65% of the rock composition, providing a relatively stable mechanical framework. Granite crystallisation typically occurs between 650-750 °C for small granitoids; therefore, significant volumetric changes are not expected at temperatures below the quartz transition under near-surface conditions. It should be noted that the α-β transition occurs at ~573 °C at atmospheric pressure, and that at greater depths, confining pressure would partially suppress thermal expansion and microcracking. However, for the purpose of this study, porosity variations below the transition can be considered negligible.

In most studies, rocks are often assumed to be homogeneous and isotropic for the sake of analytical convenience (*e.g*., Ma *et al*., 2021). However, thermal expansion and contraction are inherent physical properties that occur in response to temperature changes (Siegesmund *et al*., 2018; Lasheen and Rashwan, 2023). Differential expansion among constituent mineral grains can induce deformation and microcracking, thereby creating conditions favourable for hydrothermal mineralisation. In this context, temperature-driven changes in rocks are commonly described by either thermo-decreasing dilatancy (associated with cooling) or thermo-increasing dilatancy (associated with heating).

Thermally induced dilatancy during cooling is a characteristic feature of plutonic rocks, in which minerals crystallise at temperatures significantly higher than ambient conditions. Experimental and microstructural studies have shown that differential thermal contraction, particularly involving quartz, can generate cooling-related microcrack porosity in granitic rocks (*e.g*., Heap *et al*., 2009). For granites containing approximately 15-20% quartz, such thermally induced porosity may reach values on the order of ~1.2%, while the remaining mineral phases continue to form a mechanically coherent framework. This preservation of the external rock structure despite internal dilatancy is consistent with the development of fracture-controlled permeability in porphyry copper stockworks and episyenites developed within granitic bodies (Fig. 3).

As shown in figure 3, rock openings preferentially propagate along boundaries between quartz grains and adjacent minerals with lower thermal expansion coefficients. During cooling, the anisotropic thermal contraction of quartz relative to surrounding phases generates stress concentrations at grain boundaries and particle contacts, promoting microfracture development. This process is commonly observed around mineral inclusions, where differential thermal

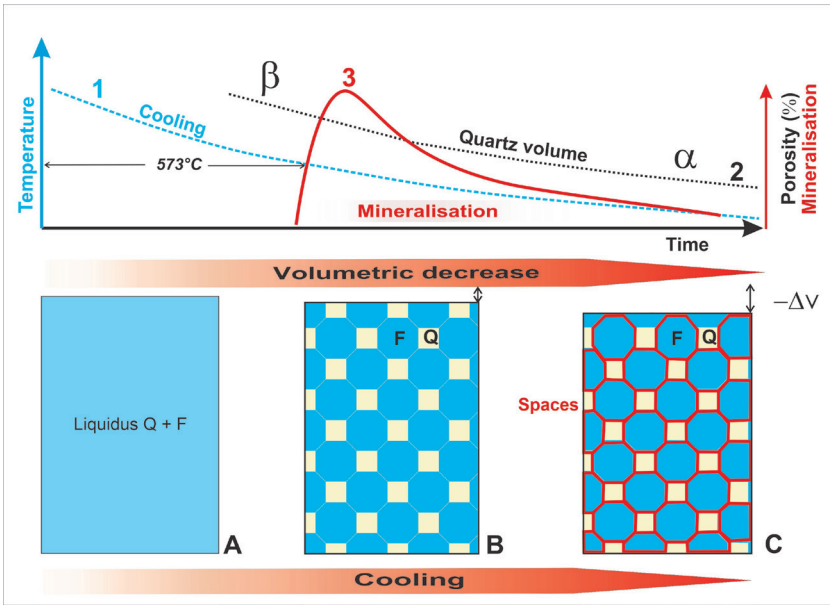


FIG. 3. Top, idealised sequence showing cooling over time (blue segmented line), quartz α-β transition (black dotted line), and emplacement of mineralization (red solid line). Bottom, schematic of differential thermal contraction in an ideal granite as temperature decreases: **1**) Cooling of a rock composed mainly of quartz (Q) and feldspar (F); **2**) Quartz contracts differently than feldspar below 573 °C; **3**) Total rock volume decreases (ΔV), creating new porosity (red lines) at the mineral grain boundaries. Panels after Rossello and López-Isaza (2023).

contraction between the host mineral and inclusions leads to the formation of radiating microcracks (Fig. 4).

An example of the link between hydrothermal evolution and microfracturing is provided by Ulrich *et al*. (2001) in their study of the Bajo de la Alumbrera porphyry Cu-Au deposit, Argentina. They documented abundant secondary fluid inclusions aligned along microfractures cutting quartz phenocrysts and feldspars, indicating repeated brittle failure and subsequent sealing by quartz precipitation. Such fracture-seal textures reflect transient microscale permeability generated during cooling and evolving stress conditions. Similar processes have since been widely documented using cathodoluminescence imaging, revealing multiple generations of healed quartz microfractures and late-stage quartz growth associated with episodic deformation and fluid flow (*e.g*., Carter *et al*., 2021; Carter and Williamson, 2022). Together, these studies demonstrate that microfracturing and subsequent quartz sealing are important mechanisms controlling permeability during hydrothermal evolution.

On the other hand, rocks can also be subject to increasing temperatures due to compaction, metamorphism or heating in proximity to plutonic intrusions. Rocks with high quartz content (*e.g*., quartzite, sandstone), as well as water-saturated rocks, are considered the best heat conductors (Schön, 2015). Water adheres to fractured grain boundaries and damaged minerals and then increases the thermal capacity of the rock (Wu *et al*., 2021). In the case of sedimentary rocks, secondary heating can cause a greater expansion of quartz grains with respect to the less thermally active feldspars, disturbing the physical structure and enhancing openings and developing microfractures. Volume changes due to heating would therefore be strongly dependent on the mineral assemblage and the original structure of the rock (Tripathi *et al*., 2024)

Thermal effects on monomineralic rocks are primarily influenced by the crystallographic orientation and the anisotropic expansion coefficient of the minerals. Depending on the temperature intensity, thermal cracking can occur either between adjacent grains or within individual grains (Yavuz *et al*., 2010). For example, in monocrystalline quartz, a strong correlation exists between the rate of expansion and the crystal orientation. Thermal expansion

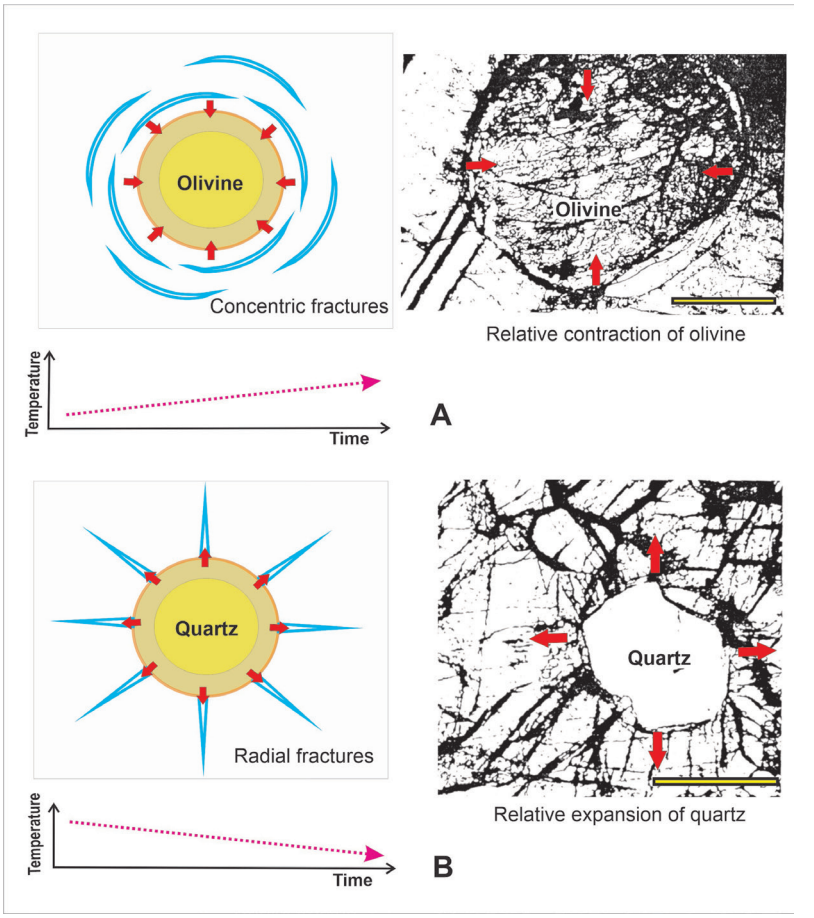


FIG. 4. Photomicrographs of (**A**) olivine inclusion within feldspar causing concentric annular fractures, and (**B**) quartz inclusion in clinopyroxene causing radial fractures (after Van der Molen and Van Roermund, 1986). Scale bars=100 μm. Sketches representing fracturing patterns and temperature changes for each case are also shown.

increases with temperature along directions parallel to the crystallographic axes, with a sharp increase near the phase transition. Additionally, the linear compressibility of α-quartz is greater in the direction parallel to the c-axis (Raz *et al*., 2002).

4. Discussion

Variations in plutonic rock textures reflect changes in magma evolution, emplacement depth, and fluid behaviour, making them a valuable record of magmatic-hydrothermal processes. In this context, magmas crystallising at greater crustal depths generally develop relatively uniform, equigranular textures, reflecting stable crystallisation conditions (Candela, 1997; Carter and Williamson, 2022). By comparison, intrusive rocks linked to magmatic-hydrothermal mineral systems commonly display far more intricate textural characteristics. The end-product of these intrusions are frequently porphyries, aplites, or pegmatites. They are often characterised by silica-rich veins, quartz phenocrysts, graphic and micrographic intergrowths, as well as dendritic, acicular, or skeletal crystal morphologies (Fenn, 1986; Kirkham and Sinclair, 1988; London and Morgan, 2012; Carter and Williamson, 2022). Such textures record the influence of multiple interacting physical and chemical processes that promote magmatic-hydrothermal mineralisation, including progressive magma evolution toward water- and metal-enriched compositions (Rohrlach and Loucks, 2005), along with rapid fluid ascent that induces undercooling

and volatile exsolution (Candela, 1997; Richards, 2005; Sillitoe, 2010; Wilkinson, 2013).

As previously noted, differential thermal expansion of minerals potentially affects the rock permeability, creating more favourable conditions for fluids mobilisation and ore emplacement. Rock permeability usually ranges from ~10^{-10} m^2 in fractured igneous and metamorphic rocks to ~10^{-20} m^2 in competent, unfractured units (Lowell *et al*., 1993). Estimates of mean permeability in hydrothermal systems tend to range between 10^{-11} to 10^{-16} m^2, indicating the influence of fractures in these environments (Lowell *et al*., 1993).

Quartz solubility increases with pressure at all temperatures (Seward *et al*., 2013; Fig. 5). Mineral expansion and the concomitant system decompression would reduce lithostatic pressure resulting in a lower solubility of silica (Candela, 1997). This will lead to a boiling effect of the residual fluid fraction, with the consequent release of gases, generally rich in mineralising elements and/or with the capacity to sweep elements from the country rock (Gao *et al*., 2024). Mineral thermal stress can therefore influence silica solubility and, ultimately, determine the rates of silica and ore precipitation in the system.

As seen in figure 5, the solubility of quartz progressively increases with temperature up to about 370 ºC. At higher temperatures the solubility becomes retrograde (*i.e*., reduction in solubility with increasing temperature). Silica dissolution initially enhances porosity and permeability, facilitating fluid flow within the rock matrix (Plümper *et al*., 2017). However, further heating to supercritical conditions induces quartz precipitation, which reduces pore space and consequently diminishes permeability, thereby restricting fluid transport (Scott and Driesner, 2018). In this context, the combined effects of grain-scale dilatancy and material removal due to rising silica solubility are major factors in the enhancement of microfractures and the growth of a crack network, facilitating the transport of fluids within the rock fabric. Experiments in polycrystalline rocks by Nurdiana *et al*. (2024), found that dissolved silica concentration in hydrothermal fluids exerts a strong control on feldspar replacement reactions and the development of secondary porosity. In that case, albite replacement was unaffected by quartz, whilst anorthite was preferentially altered when quartz was present.

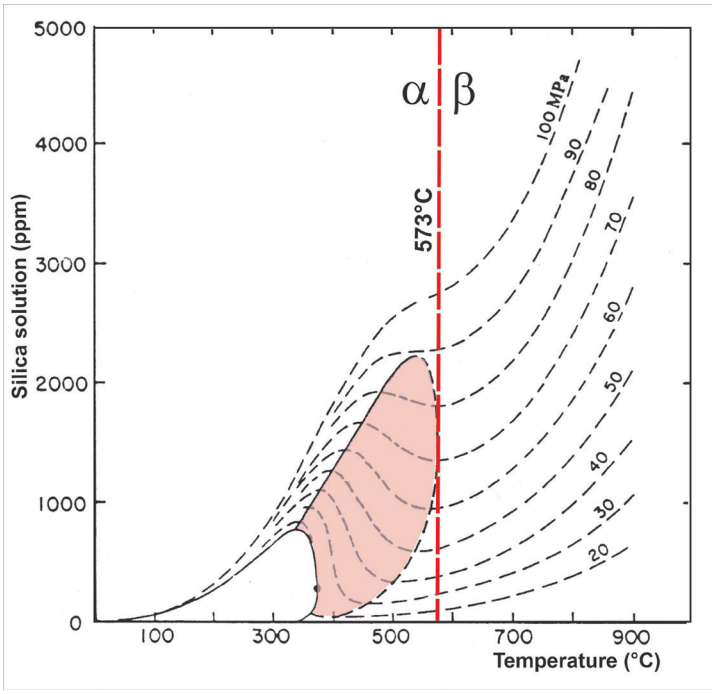


FIG. 5. Solubility of quartz in water as a function of temperature and pressure. The pink area displays the region of retrograde solubility of quartz (after Fournier and Potter, 1982 and Skinner, 1996).

Thermally induced cracks escalate with increasing temperature, predominantly as intergranular tensile cracks, followed by intragranular tensile cracks (Pan *et al*., 2024). These microfractures can evolve into a densely distributed network of interconnected flow paths, preferentially developed along grain contacts and cleavage planes (Pan *et al*., 2024). In granites, intergranular cracks are more frequent at the quartz-feldspar interface, with microcracks initiating at ~300 °C and coalescing between 400 and 600 °C (at standard atmospheric pressure). This process largely explains the sharp decrease in macroscale mechanical properties of granites (Xu *et al*., 2023). Following the initial development of these thermally induced microfractures, subsequent cooling of the rock can further influence fracture behaviour, as decreasing temperatures and fluid circulation may enhance permeability and promote the propagation or reactivation of microcracks. Under these conditions, mineral deposition becomes controlled not only by changes in fluid properties but also by the orientation of the microfractures, which guides fluid pathways and mineralisation patterns.

In porphyry deposits, stockworks of veins and veinlets are widely developed alongside hydrothermally altered zones (Liu *et al*., 2020). Thus, the distribution and abundance of the vein stockwork define the shape and geometry of the ore grade shells (Osorio *et al*., 2024). Furthermore, mineral-enriched fluids might precipitate towards the peripheries of the intrusive, where thermal variations are greatest. As a result, the spatial array of the ore would be both structurally controlled and thermally driven into the intrusive-host rock contact (Fig. 6).

Dilatant structural settings may telescope mineralisation outwards from source rocks at depth, to

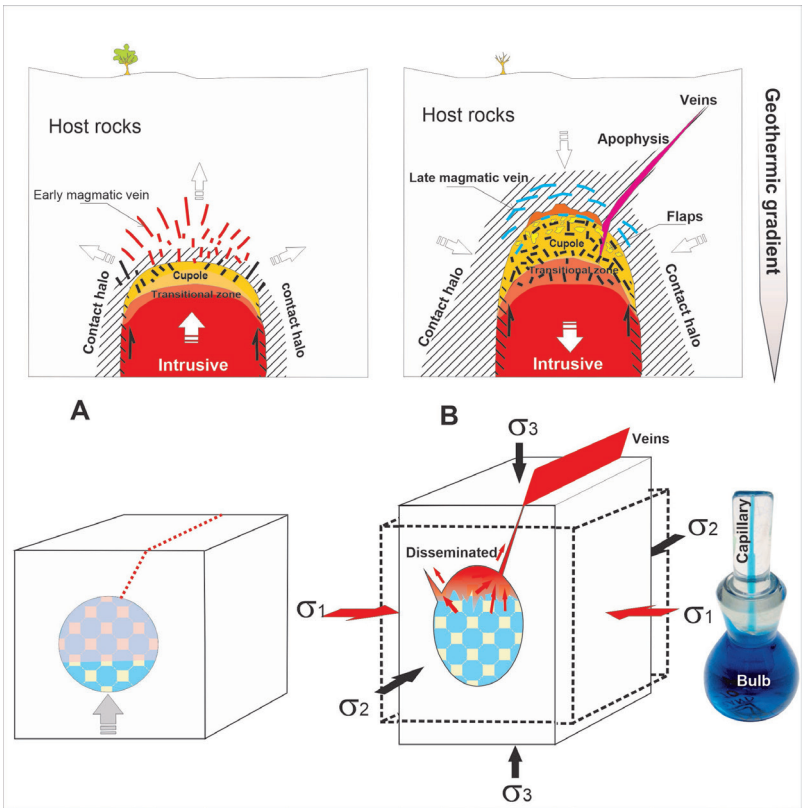


FIG. 6. Influence of thermal contraction on the formation and emplacement of mineralised bodies. **A**) Initial stage: late-stage, volatile-rich magmatic fluids concentrate near the top of the intrusive dome, forming mineralised zones between the intrusion and host rock, with thermal metamorphic halos and radially arranged veins. **B**) Final stage: fluid concentration enlarges mineralised zones and halos, with fluids escaping through a dome fault. Small volumetric changes in the magma produce strong variations along discrete fault sections, similar to how a pycnometer detects subtle changes in fluid volume (modified from Rossello and López-Isaza, 2023).

form sheeted vein related porphyry systems extending into wall rocks, or laterally and vertically to form epithermal deposits (Corbett, 2002).

5. Conclusion

Differential thermal expansion and contraction of rock-forming minerals can play a significant role in generating and enhancing preferential pathways for the migration and emplacement of mineralising fluids from igneous intrusions. Cooling of magmas during their ascent may result in ore precipitation within disseminated microfractures and cracks formed by volumetric changes at the α-β quartz transition.

The thermally induced porosity in an ideal melt of quartz and feldspars is estimated to be on the order of 1.2%, values that are consistent with observations from porphyry systems when compared with the estimated volume occupied by ore minerals. Microfractures and the opening of cracks and vacuoles would preferentially propagate along crystal boundaries, particularly at contacts between minerals with differing thermal expansion coefficients.

The volumetric expansion of the rocks can lead to fluid decompression and exsolution. This boiling effect is often associated with the release of gas phases enriched in ore components, or at least capable of mobilising elements from the surrounding wall rock. Microfracturing and the associated alteration halos may extend mineralisation outward into the host rock, ultimately producing low-grade, high-tonnage disseminated deposits.

Acknowledgements

The authors are especially grateful to Dr P.R. Cobbold† and Dr B. Reynard for their early insights and thorough discussions, which significantly contributed to the preparation of this manuscript. We also gratefully acknowledge the constructive corrections and suggestions provided by L. Carter, the Editor, and one anonymous reviewer, which greatly enhanced the clarity and understanding of our work.

References

Aoyagi, S.; Takeda, H. 2022. Transient crystal structure of oscillating quartz. *In* Novel applications of piezoelectric and thermoelectric materials (Vargas-Bernal, R.; Palma-Guerrero, R.; editors). Intech Open. https://doi.org/10.5772/intechopen.107414

Bauer, S.J.; Johnson, B. 1979. Effects of slow uniform heating on the physical properties of the Westerly and Charcoal granites. Proceedings of the 20th U.S. Symposium on Rock Mechanics: 7-18. Austin, Texas.

Boulogne, Q.; Milesi, G.; Peiffert, C.; Fischer, E.; Ballouard, C.; Serdoun, M.; Obin, T.; Lecomte, A.; Martz, P.; Kaczowka, A.; Mercadier, J. 2026. Dating circulations of hydrothermal fluids in the crystalline basement of unconformity-related metallic deposits using in situ Rb/Sr geochronology: proof of concept. EGUsphere (Preprint). https://doi.org/10.5194/egusphere-2025-6469

Brantley, S.L.; Evans, B.; Hickman, S.H.; Crerar, D.A. 1990. Healing of microcracks in quartz: Implications for fluid flow. Geology 18 (2): 136-139.

Brantut, N.; Heap, M.J.; Meredith, P.G.; Baud, P. 2013. Time-dependent cracking and brittle creep in crustal rocks: A review. Journal of Structural Geology 52: 17-43. https://doi.org/10.1016/j.jsg.2013.03.007

Breuer, S.; Schilling, F. 2021. Anisotropic thermal transport properties of quartz: from −120 °C through the α–β phase transition. European Journal of Mineralogy 33 (1): 23-38. https://doi.org/10.5194/ejm-33-23-2021

Burnham, C.W. 1979. Magmas and Hydrothermal Fluids. *In* Geochemistry of Hydrothermal Ore Deposits (Barnes, H.L.; editor), 2nd edition, John Wiley & Sons: 71-136. New York.

Burnham, W.C.; Ohmoto, H. 1980. Late-stage processes of felsic magmatism. In Granitic magmatism and related mineralization (Ishihara, S.; Takenouchi, S.; editors). Mining Geology, Special Issue No. 8: 1-11.

Candela, P.A. 1997. A review of shallow, ore-related granites: Textures, volatiles, and ore metals. Journal of Petrology 38 (12): 1619-1633. https://doi.org/10.1093/petroj/38.12.1619

Carter, L.C.; Williamson, B.J. 2022. Textural indicators of mineralisation potential in porphyry magmatic systems: A framework from the archetypal Yerington district, Nevada. Ore Geology Reviews 143: 104783

Carter, L.C.; Williamson, B.J.; Tapster, S.R.; Costa, C.; Grime, G.W.; Rollinson, G.K. 2021. Crystal mush dykes as conduits for mineralising fluids in the Yerington porphyry copper district, Nevada. Communications Earth & Environment 2: 59. https://doi.org/10.1038/s43247-021-00128-4

Chen, Z.; Su, J.W.; Ju, J.W.; Jiang, J. 2019. Experimental study on energy dissipation of fragments during rockburst. Bulletin of Engineering Geology and the Environment 78: 5369-5386. https://doi.org/10.1007/s10064-019-01463-9

Chiaradia, M. 2022. Distinct magma evolution processes control the formation of porphyry Cu-Au deposits in

thin and thick arcs. Earth and Planetary Science Letters 599: 117864. https://doi.org/10.1016/j.epsl.2022.117864

Corbett, G.J. 2002. Structural controls to porphyry Cu-Au and epithermal Au-Ag deposits. Applied Structural Geology & Mineral Exploration, Australian Institute of Geoscientists Bulletin 36: 32-35.

Ding, S.; Tang, S. 2024. Mechanical behaviour evolution and failure characteristics of saturated and dry rocks under different water pressure environments. International Journal of Rock Mechanics and Mining Sciences 178: 105777. https://doi.org/10.1016/j.ijrmms.2024.105777

Dong, L.; Zhang, Y.; Wang, L.; Zhang, S. 2024. Temperature dependence of mechanical properties and damage evolution of hot dry rocks under rapid cooling. Journal of Rock Mechanics and Geotechnical Engineering 16 (2): 645-660. https://doi.org/10.1016/j.jrmge.2023.08.014

Engvik, A.K.; Putnis, A.; Fitzgerald, J.D.; Austreim, H. 2008. Albitization of granitic rocks: The mechanisms of replacement of oligoclase by albite. The Canadian Mineralogist 46 (6): 1401-1416. https://doi.org/10.3749/canmin.46.6.1401

Fenn, P.M. 1986. On the origin of graphic granite. American Mineralogist 71 (4): 325-330.

Fournier, R.O.; Potter II, R.W. 1982. An equation correlating the solubility of quartz in water from 25° to 900 °C at pressures up to 10,000 bars. Geochimica et Cosmochimica Acta 46 (10): 1969-1973. https://doi.org/10.1016/0016-7037(82)90135-1

Frenzel, M.; Woodcock, N.H. 2014. Cockade breccia: Product of mineralisation along dilational faults. Journal of Structural Geology 68 (Part A): 194-206. https://doi.org/10.1016/j.jsg.2014.09.001

Fridovsky, V.Y.; Polufuntikova, L.I.; Kudrin, M.V. 2023. Origin of disseminated gold-sulfide mineralization from proximal alteration in orogenic gold deposits in the central sector of the Yana-Kolyma metallogenic belt, NE Russia. Minerals 13 (3): 394. https://doi.org/10.3390/min13030394

Gao, H.; Li, G.; Zhang, Z. 2024. Phase diagram and density of SiO2-H2O fluid across critical conditions. Progress in Earth and Planetary Science 11 (20): 14 p. https://doi.org/10.1186/s40645-024-00622-1

Guilbert, J.M.; Park, C.P. Jr. 2007. The geology of ore deposits. Waveland Press: 985 p.

Heap, M.J., Baud, P.; Meredith, P.G. 2009. Influence of temperature on brittle creep in sandstones. Geophysical Research Letters 36 (19): L19305. https://doi.org/10.1029/2009GL039373

Heinrich, C. 2024. The chain of processes forming porphyry copper deposits - an invited paper. Economic Geology 119 (4): 741-769. https://doi.org/10.5382/econgeo.5069

Henderson, C.M.B. 2021. Composition, thermal expansion and phase transitions in framework silicates: Revisitation and review of natural and synthetic analogues of nepheline-, feldspar- and leucite-mineral groups. Solids 2 (1): 1-49. https://doi.org/10.3390/solids2010001

Hovis, G.L.; Medford, A.; Conlon, M.; Tether, A.; Romanoski, A. 2010. Principles of thermal expansion in the feldspar system. American Mineralogist 95 (7): 1060-1068. https://doi.org/10.2138/am.2010.3484

Jiang, Z.; Yin, Q.; Wu, J.; Zhu, Q.; Li, M.; Su, H.; Jing, H. 2022. The effect of cyclic heating and cooling on mechanical and deformation responses of granites under preset angle shearing. Environmental Earth Sciences 82 (29). https://doi.org/10.1007/s12665-022-10711-3

Johnson, S.E.; Song, W.J.; Cook, A.C.; Vel, S.S.; Gerbi, C.C. 2021. The quartz α↔β phase transition: Does it drive damage and reaction in continental crust? Earth and Planetary Science Letters 553: 116622. https://doi.org/10.1016/j.epsl.2020.116622

Kirkham, R.V.; Sinclair, W.D. 1988. Recent advances in the geology of granite-related mineral deposits. *In* Proceedings of the CIM Conference on Granite-related Mineral Deposits, (Taylor, R.P.; Strong, D.F.; editors). Canadian Institute of Mining and Metallurgy, Special volume 31: 50-71.

Kiss, D.; Moulas, E.; Kaus, B.J.P.; Spang, A. 2023. Decompression and fracturing caused by magmatically induced thermal stresses. Journal of Geophysical Research: Solid Earth 128 (3): e2022JB025341. https://doi.org/10.1029/2022JB025341

Korges, M.; Weis, P.; Andersen, C. 2020. The role of incremental magma chamber growth on ore formation in porphyry copper systems. Earth and Planetary Science Letters 552: 116584. https://doi.org/10.1016/j.epsl.2020.116584

Kozu, S.; Ueda, J. 1933. Thermal expansion of plagioclase. Proceedings of the Imperial Academy of Tokyo 9 (6): 262-264.

Kroll, H. 1984. Thermal Expansion of Alkali Feldspars. *In* Feldspars and Feldspathoids (Brown, W.L.; editor). Springer, NATO ASI Series, vol. 137. Dordrecht. https://doi.org/10.1007/978-94-015-6929-3_5

Kumar, S. 2014. Magmatic processes: review of some concepts and models. Modelling of magmatic and allied processes: 1-22. https://doi.org/10.1007 978-3-319-06471-0_1

Lasheen, E.S.R.; Rashwan, M.A. 2023. Effect of mineralogical variations on physic-mechanical and thermal properties of granitic rocks. Scientific Reports 13: 10320. https://doi.org/10.1038/s41598-023-36459-9

Liu, R.; Chen, G.; Yang, J. 2020. Compositions of Cu-(Fe)-sulfides in the 109 reduced granite-related Cu deposit, Xinjiang, Northwest China: Implications for the characteristics of ore-forming fluids. Geofluids: 7391369. https://doi.org/10.1155/2020/7391369

Lowell, R.P.; Van Cappellen, P.; Germanovich, L.N. 1993. Silica precipitation in fractures and the evolution of permeability in hydrothermal upflow zones. Science 260: 192-194. https://doi.org/10.1126/science.260.5105.192

London, D.; Morgan, G.B. 2012. The pegmatite puzzle. Elements 8 (4): 263-268. https://doi.org/10.2113/gselements.8.4.263

Ma, Z.; Zhang, G.; Gamage, R.P.; Zhang, C.H. 2021. Measurement of thermal expansion coefficient of rock minerals using XRD and its implications to thermal damage mechanism. IOP Conference Series: Earth and Environmental Science 861 (7): 072021. https://doi.org/10.1088/1755-1315/861/7/072021

Mavrogonatos, C.; Voudouris, P.; Spry, P.G.; Melfos, V.; Klemme, S.; Berndt, J.; Baker, T.; Moritz, R.; Bissig, T.; Monecke, T. 2018. Mineralogical study of the advanced argillic alteration zone at the Konos Hill Mo-Cu-Re-Au porphyry prospect, NE Greece. Minerals 8 (11): 479. https://doi.org/10.3390/min8110479

McCann, K. 2024. The origin of propylitic alteration halos in porphyry systems. UK Research and Innovation. https://gtr.ukri.org/projects?ref=studentship-2607407

Mcmillan, W.J.; Panteleyev, A. 1998. Porphyry copper deposits. *In* Ore deposit models, Geoscience Canada (Roberts, R.G.; Sheahan, P.A.; editors). Reprint Series 3: 45-58.

Misra, K.C. 2000. Porphyry deposits. *In* Understanding Mineral Deposits, Chapter 8. Springer, Dordrecht. https://doi.org/10.1007/978-94-011-3925-0_8

Mittal, T.; Richards, M.A. 2019. Volatile Degassing From Magma Chambers as a Control on Volcanic Eruptions: Journal of Geophysical Research: Solid Earth 124(8): 7869-7901. https://doi.org/10.1029/2018JB016983

Norberg, N.; Neusser, G.; Wirth, R.; Harlov, D. 2011. Microstructural evolution during experimental albitization of K-rich alkali feldspar. Contributions to Mineralogy and Petrology 162: 531-546.

Nurdiana, A.; Okamoto, A.; Uno, M.; Tsuchiya, N. 2024. Porosity generation via spatially uncoupled dissolution-precipitation during plagioclase replacement in quartz undersaturated fluids. Contributions to Mineralogy and Petrology 179: 10. https://doi.org/10.1007/s00410-023-02088-8

Osorio, J.; Dilles, J.H.; Collao, S. 2024. Fluid and vein evolution, timing, and temperature of Cu-Au-Mo sulfide deposition at the Encuentro Porphyry Cu-Au-Mo Deposit, Northern Chile. Economic Geology 119 (6): 1289-1328. https://doi.org/10.5382/econgeo.5088

Pacey, A.; Wilkinson, J.J.; Cooke, D.R. 2020. Chlorite and epidote mineral chemistry in porphyry ore systems: A case study of the Northparkes District, New South Wales, Australia. Economic Geology 115 (4): 701-727. https://doi.org/10.5382/econgeo.4700

Pan, J.; Ma, Y.; Zhang, L.; Xi, X.; Zhang, Y.; Cai, M. 2024. Effect of heat treatment on microcracking behaviours and Mode-I fracture characteristics of granite: An experimental and numerical investigation. Theoretical and Applied Fracture Mechanics 132: 104489. https://doi.org/10.1016/j.tafmec.2024.104489

Phillips, G.N.; Vearncombe, J.R.; Clemens, J.D.; Day, A.; Kisters, A.F.M. 2023. Formation of Cu-Au porphyry deposits: Hydraulic quartz veins, magnetic processes and constraints from chlorine. Australian Journal of Earth Sciences 70 (7): 1010-1033. https://doi.org/10.1080/08120099.2023.2237105

Plümper, O.; Botan, A.; Los, C.; Liu, Y.; Malthe-Sørenssen, A.; Jamtveit, B. 2017. Fluid-driven metamorphism of the continental crust governed by nanoscale fluid flow. Nature Geoscience 10 (9): 685-690. https://doi.org/10.1038/ngeo3009

Qiu, L.; Xie, L.; Qin, Y.; Wang, J.; Liu, S.; Qian, J. 2024. Study on mechanical properties of interbedded rock masses with microcracks based on thermal-mechanical coupling. PLoS ONE 19 (2): e0280486. https://doi.org/10.1371/journal.pone.0280486

Raman, C.; Nedungadi, T. 1940. The α-β transformation of quartz. Nature 145: 147. https://doi.org/10.1038/145147a0

Raz, U.; Girsperfer, S.; Thompson, A. 2002. Thermal expansion, compressibility and volumetric changes of quartz obtained by single-crystal dilatometry to 700 °C and 3.5 kilobars (0.35 GPa). Swiss Journal of Geosciences Supplement 82 (3): 561-574.

Richards, J.P. 2005. Cumulative factors in the generation of giant calc-alkaline porphyry Cu deposits. *In* Super porphyry copper and gold deposits: A global perspective (Porter, T.M.; editor), v. 1, Porter Geoscience Consulting Publishing 7-25. Adelaide.

Rohrbach, B.; Loucks, R. 2005. Multi-million-year cyclic ramp-up of volatiles in a lower crustal magma reservoir trapped below the Tampakan copper-gold deposit by Mio-Pliocene crustal compression in the southern Philippines. Porter Geoscience Consulting Publishing 2: 369-407. Adelaide.

Rossello, E.A. 2008. Thermo-tectonic control in the emplacement of mineralisation: A work hypothesis. Revista de Geociências (São Paulo, Brasil) 26 (3): 191-201.

Rossello, E.A.; Reynard, B. 1997. Primary porosity in granitic rocks due to differential thermal expansivity of quartz and feldspars at the α-β quartz transition. International Symposium on Granites and Associated Mineralizations No. 2: Abstract 151. Salvador, Brazil.

Rossello, E.A.; López-Isaza, J.A. 2023. The structural control of mineralisations by dilatancies due to differential thermal expansivity (in disseminated deposits) and faults bending (in veins): Revision and working hypothesis. Revista Mexicana de Ciencias Geológicas 40 (1): 16-34. https://doi.org/10.22201/cgeo.20072902e.2023.1.1716

Ruiz, Y.; Zhang, L.S.; Wu, C.Y.; Wang, L.S.; Sun, X.Y. 2005. Dexing porphyry copper deposits in Jiangxi, China. *In* Porphyry and hydrothermal copper and gold deposits: A global perspective (Porter, T.M.; editor). Porter Geoscience Consulting Publishing: 409-421. Adelaide.

Schön, J.H. 2015. Physical properties of rocks: Fundamentals and principles of petrophysics (2nd edition). Developments in Petrophysics 65: 499 p.

Scott, S.W.; Driesner, T. 2018. Permeability changes resulting from quartz precipitation and dissolution around upper crustal intrusions. Geofluids 19: 6957306. https://doi.org/10.1155/2018/6957306

Seedorff, E.; Dilles, J.H.; Proffett, J.M.Jr.; Einaudi, M.T.; Zurcher, L.; Stavas, W.J.A.; Johnson, D.A.; Barton, M.D. 2005. Porphyry deposits: Characteristics and origin of hypogene features. *In* 100th Anniversary Volume (Hedenquist, J.W.; Thompson, J.F.H.; Goldfarb, R.J.; Richards, J.P.; editors). Society of Economic Geologists: 251-298. https://doi.org/10.5382/AV100.10

Seedorff, E.; Barton, M.D.; Stavast, W.J.A.; Maher, D.J. 2008. Root zones of porphyry systems: Extending the porphyry model to depth. Economic Geology 103 (5): 939-956. https://doi.org/10.2113/gsecongeo.103.5.939

Seward, T.M.; Migdisov, A.; Williams-Jones, A.E. 2013. The chemistry of metal transport and deposition by ore-forming hydrothermal fluids. *In* Treatise on Geochemistry, Geochemistry of Mineral Deposits, vol. 13 (Holland, H.; Turekian, K.; editors). Elsevier: 29- 57. Amsterdam. https://doi.org/10.1016/B978-0-08-095975-7.01102-5

Shao, S.; Ranjith, P.G.; Wasantha, P.L.P.; Chen, B.K. 2015. Experimental and numerical studies on the mechanical behaviour of Australian Strathbogie granite at high temperatures: An application to geothermal energy. Geothermics 54: 96-108. https://doi.org/10.1016/j.geothermics.2014.11.005

Siegesmund, S.; Sousa, L.; Knell, C. 2018. Thermal expansion of granitoids. Environmental Earth Sciences 77 (2). https://doi.org/10.1007/s12665-017-7119-2

Sillitoe, R.H. 2000. Gold-rich porphyry deposits: Descriptive and genetic models and their role in exploration and discovery. *In* Gold in 2000, vol. 13 (Hagemann, S.G.; Brown, P.E.; editors). Society of Economic Geologists: 315-345. https://doi.org/10.5382/REV.13.09

Sillitoe, R.H. 2010. Porphyry copper systems. Economic Geology 105 (1): 3-41. https://doi.org/doi:10.2113/gsecongeo.105.1.3

Sinclair, W.D. 1995. Vein-Stock tin, tungsten. Geology of Canadian Mineral Deposit Types. *In* Geological Society of America (Eckstrand, O.R.; Sinclair, W.D; Thorpe, R.I,K.; editors). https://doi.org/10.1130/DNAG-GNA-P1

Skinner, B.J. 1966. Thermal expansion. *In* Handbook of Physical Constants (Clark, Jr, S.P.; editor). Geological Society of America Memoir 97: 75-96.

Sly, M.K.; Padilla, K.; Flores, K.M.; Skemer, P. 2023. Low-temperature plastic rheology of granitic feldspar and quartz. Tectonophysics 858 (1): 229850. https://doi.org/10.1016/j.tecto.2023.229850

Smirnov, V.I. 1976. Geology of mineral deposits. Mir Publishers, Moscow: 356 p.

Sokolar, R.; Nguyen, M. 2024. Anorthite ceramics: Grog and clay selection for lowering the sintering temperature. Journal of the Asian Ceramic Society 12 (2): 129-140. https://doi.org/10.1080/21870764.2024.2320448

Stanton-Yonge, A.; Sánchez de la Muela, A.; Pearce, R.K.; Hammond, J.O.S.; Mitchell, T.M.; Hicks, S.P.; Griffith, W.A.; Moorkamp, M.; Meredith, P.G.; Cembrano, J. 2025. Fluid pressure fluctuations and the seismic signature of a fault-controlled fluid migration pulse. Earth and Planetary Science Letters 662: 119388. https://doi.org/10.1016/j.epsl.2025.119388

Streckeisen, A. 1974. Classification and nomenclature of plutonic rocks. Geologische Rundschau 63: 773-786.

Tosdal, R.M.; Richards, J.P. 2001. Magmatic and structural controls on the development of porphyry Cu±Mo±Au deposits. *In* Structural controls on ore genesis (Richards, J.P.; Tosdal, R.M.; editors). Society of Economic Geologists Vol. 14: 157-181.

Tribaudino, M.; Angel, R.J.; Cámara, F.; Nestola, F.; Pasqual, D.; Margiolaki, I. 2010. Thermal expansion of plagioclase feldspars. Contributions to Mineralogy and Petrology 160 (6): 899-908. https://doi.org/10.1007/s00410-010-0513-3

Tripathi, A.; Khan, M.M.; Pain, A.; Rai, N.; Iqbal, M.A. 2024. Experimental study on the quasi-static and dynamic tensile behaviour of thermally treated Barakar sandstone in Jharia coal mine fire region, India. Scientific Reports 14 (5270). https://doi.org/10.1038/s41598-024-54199-2

Ulrich, T.; Günther, D.; Heinrich, C.A. 2001. The evolution of a porphyry Cu-Au deposit, Bajo de la Alumbrera, Argentina: Fluid inclusion and isotope evidence. Economic Geology 96 (8): 1719-1742.

Van der Molen, I.; Van Roermund, H.L.M. 1986. The pressure path of solid inclusions in minerals: The retention of coesite inclusions during uplift. Lithos 19 (3-4): 317-324. https://doi.org/10.1016/0024-4937(86)90030-7

Vázquez, P.; Benavente, D.; Montiel, D.; Gómez-Heras, M. 2021. Mineralogical transformations in granitoids during heating at fire-related temperatures. Applied Sciences 12 (1): 188. https://doi.org/10.3390/app12010188

Vázquez, P.; Shushakova, V.; Gómez-Heras, M. 2015. Influence of mineralogy on granite decay induced by temperature increase: Experimental observations and stress simulation. Engineering Geology 189: 58-67. https://doi.org/10.1016/j.enggeo.2015.01.026

Vigneresse, J.L. 2007. The role of discontinuous magma inputs in felsic magma and ore generation. Ore Geology Reviews 30 (3-4): 181-216. https://doi.org/10.1016/j.oregeorev.2006.03.001

Wilkinson, J.J. 2013. Triggers for the formation of porphyry deposits in magmatic arcs. Nature Geoscience 6 (11): 917-925. https://doi.org/10.1038/ngeo1940

Wu, X.; Guo, Q.; Zhu, Y.; Ren, J.; Zhang, J.; Wu, X.; Cai, M. 2021. Pore structure and crack characteristics in high-temperature granite under water-cooling. Case Studies in Thermal Engineering 28: 101646. https://doi.org/10.1016/j.csite.2021.101646

Xu, X.Y.; Xu, X.C.; Xie, Q.Q.; Fu, Z.Y.; Lu, S.M.; Zhao, L.L. 2022. Geological features and ore-forming mechanisms of the Chating Cu-Au deposit: A rare case of porphyry deposit in the Middle-Lower Yangtze River metallogenic belt. Ore Geology Reviews 144: 104860. https://doi.org/10.1016/j.oregeorev.2022.104860

Xu, J.J.; Zhang, Y.H.; Rutqvist, J.; Hu, M.S.; Wang, Z.Z.; Tang, X.H. 2023. Thermally induced microcracks in granite and their effect on the macroscale mechanical behaviour. Journal of Geophysical Research: Solid Earth 128 (1): e2022JB024920. https://doi.org/10.1029/2022JB024920

Xu, Y.; Xie, F.; Cao, R.; Zhou, A.; Sun, Y.; Zhang, J.; Qiao, F.; Qiu, Z.; Liu, S. 2025. Episodic hydrothermal pulses controlling skarn copper mineralization in the Secuo deposit, Xizang: Insights from in situ garnet geochemistry and chronology. Ore Geology Reviews 184: 106734. https://doi.org/10.1016/j.oregeorev.2025.106734

Yavuz, H.; Demirdag, S.; Caran, S. 2010. Thermal effect on the physical properties of carbonate rocks. International Journal of Rock Mechanics and Mining Sciences 47 (1): 94-103. https://doi.org/10.1016/j.ijrmms.2009.09.014

Zhang, S.; He, W.; Wang, H.; Xiao, Y. 2025. Thermodynamic modelling constrains the alteration and mineralization patterns of the Pulang Porphyry Cu-Au Deposits in Eastern Tibet. Minerals 15 (8): 780. https://doi.org/10.3390/min15080780

Manuscript received: April 11, 2025; revised/accepted: February 06, 2026; available online: February 06, 2026.